Detecting and quantifying zero tillage technology adoption in Indian smallholder systems using Sentinel-2 multi-spectral imagery

Article · March 2024

DOI: 10.1016/j.jag.2024.103779

Vijesh V Krishna
CIMMYT

International Journal of Applied Earth Observation and Geoinformation 128 (2024) 103779

Contents lists available at ScienceDirect

International Journal of Applied Earth Observation and Geoinformation

journal homepage: www.elsevier.com/locate/jag

Detecting and quantifying zero tillage technology adoption in Indian smallholder systems using Sentinel-2 multi-spectral imagery

Monish Vijay Deshpande [a,b], Dhanyalekshmi Pillai [a,b,*], Vijesh V. Krishna [c], Meha Jain [d]

[a] *Indian Institute of Science Education and Research Bhopal (IISERB), Bhopal, India*
[b] *Max Planck Partner Group (IISERB), Max Planck Society, Munich, Germany*
[c] *CIMMYT, Sustainable Agrifood Systems (SAS) Program, Hyderabad, India*
[d] *School for Environment and Sustainability, University of Michigan, Ann Arbor, MI, USA*

ARTICLE INFO

Keywords:
Zero tillage
Sentinel-2
Conservation agriculture
Google Earth Engine
Random forest

ABSTRACT

Zero tillage (ZT), an important component of Conservation Agriculture, has enormous potential to curb emissions from residue burning, increase soil organic carbon and water retention, reduce land preparation costs and increase the long-term productivity and profitability of the farming system. Despite the promise of ZT, little is known about how widely it has been adopted at regional scales in smallholder systems, where management is heterogeneous. Identifying ZT diffusion patterns across space and time along with other popular tillage technologies, such as conventional tillage (CT) and shallow tillage (ST), helps to target and disseminate the most effective technologies and estimate their climate change mitigation potential. Acknowledging the complexities involved in distinguishing ZT from CT and ST in smallholder fields, this study utilized an innovative two-step change detection method leveraging early-season Sentinel-2 multi-spectral imagery. We developed and applied our model in the Indian state of Punjab over three years (2020–2022). Our method outperformed traditional binary classification models, achieving 81 % accuracy. The analysis indicated that areas under different tillage types changed over time across Punjab. Specifically, from 2020 to 2021, we found a 33 % and 4 % decrease in ZT and CT, respectively. However, a 29 % increase is observed in CT adoption. On the other hand, from 2021 to 2022, the adoption rates for ZT and CT increased by 18 % and 2 %, respectively, while ST adoption decreased by 12 %. Overall, this study demonstrates the potential use of early season Sentinel-2 imagery to map the adoption of tillage practices in smallholder systems. Our approach can provide large-scale information on technology uptake, aiding policies to implement carbon markets and the scaling up of sustainable agricultural practices in India.

1. Introduction

Conservation Agriculture (CA) constitutes a set of principles and practices that maintain soil structure and fertility while improving yield and profits (El-Shater et al., 2020) and is promoted by the United Nations Food and Agriculture Organization (FAO) and various other international development organizations. Zero tillage (ZT) involves field preparation with minimal soil disturbance, often by directly planting seeds in residues retained from the previous crop harvest (Kassam et al., 2009; Chabert and Sarthou, 2020). While ZT is widely adopted in many developed countries, its implementation is limited in developing nations, even though it has been shown to have advantages over conventional practices (Stewart et al., 2008; Krishna et al., 2022). While ZT use is increasing in many agricultural systems worldwide, there is a lack of knowledge regarding the scale of its adoption at the regional and national levels (Krishna et al., 2022). This gap is especially pronounced in smallholder farming systems like those in India, where information about tillage practices is often unavailable through ground or census data (Jat et al., 2020).

Historically, information about tillage use has been collected through survey-based methods, yet doing so is expensive and time-consuming, making it impractical to use across large areas (Watts et al., 2011; Azzari et al., 2019; Kubitza et al., 2020). Satellite-based tillage mapping has been proposed as a way to produce large-scale tillage data, at the field scale, and annually (Lal, 2005; Watts et al., 2011; Azzari et al., 2019; Kubitza et al., 2020; Zhou et al., 2021).

* Corresponding author at: Indian Institute of Science Education and Research Bhopal (IISERB), Bhopal, India.
E-mail address: dhanya@iiserb.ac.in (D. Pillai).

https://doi.org/10.1016/j.jag.2024.103779
Received 10 November 2023; Received in revised form 5 February 2024; Accepted 17 March 2024

Previous studies have used satellite data to classify tillage practices and also the percent of crop residue cover (CRC) (Luotamo et al., 2022; Hively et al., 2018; Ding et al., 2020; Gao et al., 2022). Many of these studies have found that CRC can be detected with optical reflectance, with some studies emphasizing the significance of the shortwave-infrared (SWIR) spectrum (ranging from 2100 to 2400 nm) in distinguishing crop residues from soil background soils (Daughtry et al., 2004; Daughtry et al., 2006; Bricklemyer et al., 2006; Azzari et al., 2019; Sharma et al., 2016).

Previous studies that have conducted satellite-based mapping of tillage practices have predominantly used Landsat satellite data (Azzari et al., 2019; Zheng et al., 2012). Though Landsat can be used for mapping cultivation techniques in regions characterized by large fields, such as in the United States, it may not be adequate for mapping individual fields in smallholder systems due to its coarse spatial resolution of 30 m (Zheng et al., 2013; Jain et al., 2016; Azzari et al., 2019; Sharma et al., 2016). Recent high spatial-resolution satellite retrievals, such as those from Sentinel-2 (10 m), can potentially improve tillage mapping in smallholder fields. Tillage classification can be improved using high-resolution data, which reduces the chance of mixed pixels (Watts et al., 2011). Furthermore, three red-edge bands of Sentinel-2 can improve agricultural land cover classification accuracies (Immitzer et al., 2016; Xie et al., 2019; Zhou et al., 2021). However, only a few studies have mapped CRC using Sentinel-2 data, and fewer have classified tillage practices using Sentinel-2 data (Ding et al., 2020; Zhou et al., 2021; Liu et al., 2022). Those that have used Sentinel-2 data to classify smallholder tillage adoption have done so to classify only binary categories, ZT and conventional tillage (CT), missing alternative tillage practices, such as shallow tillage (ST), that are prevalent in smallholder systems (Zhou et al., 2021; Liu et al., 2022).

Multi-temporal satellite imagery is advantageous for delineating agricultural features (Daughtry et al., 2005; Serbin et al., 2009; Zheng et al., 2012; Zheng et al., 2014). Previous studies have highlighted the importance of image acquisition time for classifying tillage adoption, particularly imagery early in the growing season (Quemada et al., 2018; Azzari et al., 2019; Hively et al., 2018; Kubitza et al., 2020; Zhou et al., 2021; Gao et al., 2022). However, satellite imagery before the start of the growing season can also be important for classifying tillage practices, as ZT and CT fields differ in their crop residue management. In ZT fields, crop residues can be retained, while in CT fields, the residues are removed or burned. In particular, such differences can be detected best during the period when the prior crop is harvested through the end of sowing of the crop for which the tillage practice is being classified (Lewis et al., 2006; Zhou et al., 2021). In addition, by using early-season imagery, tillage maps could be produced at the start of the growing season, providing reliable and timely within-season information about adoption to policymakers and stakeholders.

In this study, we focus on ZT mapping in India using Sentinel-2 satellite data, Google Earth Engine (GEE), and a random forest classifier for three years (2020–2022). Our study addresses the complex issue of classifying diverse tillage practices adopted in a heterogeneous smallholder system, Punjab, India, using a novel modified change detection approach and early season imagery. Specifically, we assess the accuracy of classifying ZT, CT, and ST (which is performed using a tillage machine called the Super Seeder) across the state and in multiple years. This study is important because it provides the first classification of multiple tillage types, including ST, in smallholder systems and investigates the efficacy of generating precise classification models with minimal training data. As an outcome of our study, we develop a cost-effective remote sensing-based approach that can be useful for researchers and policymakers in tracking the adoption of ZT over large spatiotemporal scales. Such information is crucial to better understand the effectiveness of different policies and interventions that have been conducted to increase ZT adoption and to estimate associated carbon mitigation.

2. Materials and methods

2.1. Study region and characteristics

Being the largest wheat and rice-producing state in India, we have chosen the entire state of Punjab for our case study. Punjab (central latitude/longitude: 31.1471°N/75.3412°E) is recognized for its significant contribution to the country's annual agricultural output, with wheat (10 million tons), rice (11 million tons), sugarcane (2 million tons), and cotton (1 million tons) being the major crops grown (Agricultural Statistics at Glance, 2021). Fig. 1 details the extent of the study area, sample district, village and field locations where ground truth data were collected, and field images. Punjab's agro-climate is characterized by a semi-arid environment with hot summers and dry cold winters, where most of its rainfall occurs during the monsoon season, from July to September. The state's soil type is predominantly alluvial, well-suited for agriculture, and highly fertile. Nearly 98 % of cultivable land in Punjab is under irrigation, including canal irrigation, tube wells, and drip irrigation, supported by a well-developed irrigation system that promotes crop cultivation throughout the year. Typically, rice is grown during the monsoon season (from June to September), and wheat is grown during the winter season (from November to April).

Since early 2000, the state government of Punjab has been promoting the widespread adoption of ZT for wheat and rice production by

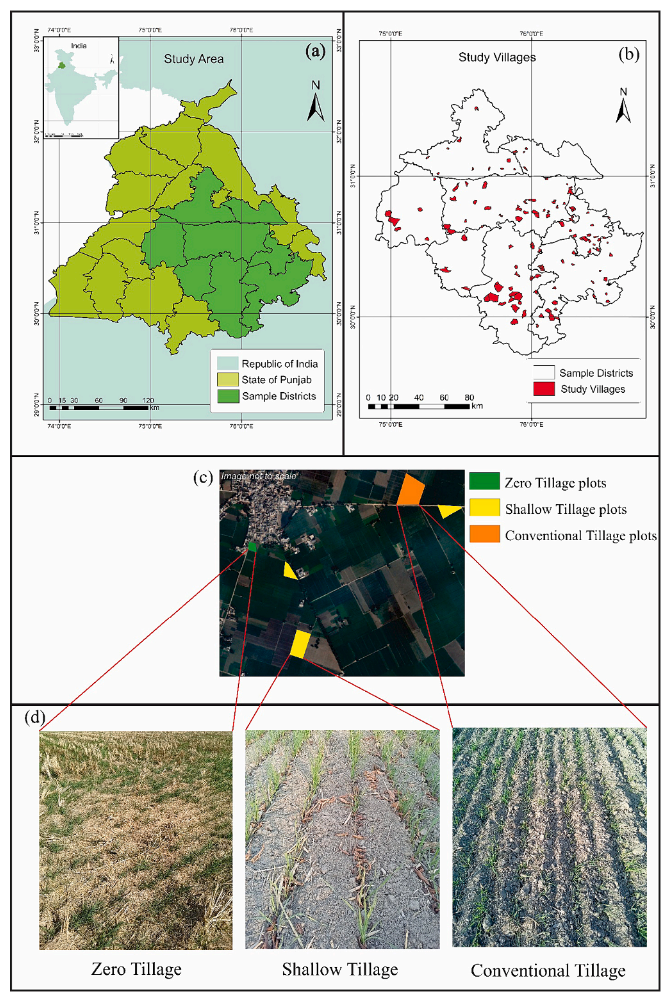

Fig. 1. (a) Study area, state of Punjab, location in reference to India. (b) Study area with locations of sample villages selected for ground truth survey. (c) Ground truth sample plots overlaid on high-resolution satellite images for November 2022 in Google Earth and (d) showing the field conditions of respective tillage adoption observed during the survey. (2 column image).

providing various subsidies and innovations, resulting in 0.41 Million Hectares (Mha) under ZT by 2006 (Tiwari et al., 2010). However, despite the government's initiatives to popularise ZT, many surveys suggest that most farmers still prefer to use conventional tillage methods, although ST is gaining in popularity. ST is practised using the Super Seeder machine, which incorporates rice residues into the soil in a single tractor pass, concurrently ensuring a finely prepared seedbed and the sowing of wheat, which makes the process less tillage-intensive than CT (Singh et al., 2023). CT is much easier to adopt compared to ST and ZT, with readily available machinery and inexpensive residue removal options, primarily through burning (El-Shater et al., 2016). We focus on mapping tillage practices adopted when planting the winter crop, wheat, as this is the crop that has the largest area under ZT or ST in Punjab.

2.2. Ground truth data

We conducted the field survey and collected ground truth data after the monsoon harvest. A key informant survey was carried out in 2022 from a total of 122 villages from eight districts of Punjab to examine the aggregate adoption levels of different tillage practices in the sample villages. The selection of villages was conducted in two stages. In 2018, 52 villages were initially selected from four districts (Fatehgarh Sahib, Ludhiana, Patiala, and Sangrur) based on the presence of at least one Happy Seeder (HS) user. Subsequently, an additional 70 villages were randomly added to the sample from another four wheat-growing districts (Bernala, Jalandhar, Moga, and Shahid Bhagat Singh Nagar) in the 2022 survey. From each selected village, one expert farmer participated in the key informant survey, providing insights on various aspects such as village characteristics, cropping patterns, technology adoption details, residue management strategies, groundwater availability, different soil types, and other resource conservation practices followed by farmers in the village. The technology adoption details included information about monsoon crop harvesting dates, winter crop sowing dates, and tillage practices, specifically the area under CT, ZT, or ST.

We also collected georeferenced plots of different tillage types from these villages that we could use to train and validate our remote sensing algorithm. We employed stratified sampling to collect plots with CT, ZT, and ST, sampling three to four plots from each of the 122 villages, totalling 426 plots. Three trained enumerators recorded the tillage type based on visual inspection of the field and took photographs of the field in case they needed additional input to verify the tillage type. This effort resulted in data for 137 plots under CT, 144 plots under ST and 145 plots under ZT (Fig. 1a,b). The data included GPS locations at the four corners and centre of the plots, which were later used to create the plot polygons. We overlaid the created polygons on high-resolution imagery in Google Earth and adjusted plot boundaries as needed to match those seen in the high-resolution imagery. The Google Earth images closest to the survey dates were used to ensure consistency between the surveyed plot boundaries and the visible boundaries in the imagery. Fig. 1c shows the sample plots overlaid on high-resolution imagery in Google Earth, and Fig. 1d depicts images of plot conditions observed for each tillage class. Form S1 gives the questionnaire used for the key informant interview and for the plot data recording.

2.3. Satellite dataset and pre-processing

We accessed the European Space Agency's (ESA) freely accessible Sentinel-2 Level 2A (S2A) product via Google Earth Engine (GEE). These data were pre-processed using the Sen2Cor algorithm, correcting for atmospheric conditions and providing surface reflectance data (Main-Knorn et al., 2017). GEE's scaling algorithm was applied to account for spatial resolution variations across spectral bands ('B2-B4' and 'B8' at 10 m and 'B6', 'B7', 'B8A', 'B11', and 'B12' at 20 m). All bands and indices were subsequently exported at 10 m resolution. Our filtering process removed S2A images with over 10 % cloud cover, and we utilized the 'QA60' band (60 m) to further mask remnants of cloud cover and shadows.

Since tillage activities are performed during the period between the end of the harvest of the monsoon crop and the pre-sowing of the winter crop, there is a strong relationship between different types of tillage practices and crop residue cover (Zheng et al., 2014). For example, fields with CT have no remaining residue cover as they get burned before tillage. In contrast, fields with ZT often have the most residue cover remaining on the field's surface. To select the early season time period that would allow us to detect such differences in crop residue cover, we referred to the harvesting and sowing calendar for our study area recorded in our survey data. We opted to create multi-date image composites instead of relying on single-date images in order to overcome the issue of missing pixels caused by cloud cover. For our analysis, we divided our early season time window into three periods: the end of the harvest, pre-sowing and post-sowing. We then created 5-day image composites for each of these three-time steps based on the date of harvest, the start date of sowing and the end date of sowing defined using the survey data. Fig. 2a depicts the sowing calendar for sample plots reported in the survey data, and Fig. 2b–d shows false colour image composites of the end of harvest, pre-sowing and post-sowing periods, respectively.

To account for the variability in agricultural fields and tillage methods, we examined various indices tailored for tillage detection in addition to chlorophyll indices. Our analysis encompassed three visual spectrum bands (B2–B4), a near-infrared (NIR) band (B8), three red-edge bands (B6–B7, and B8A), a SWIR-1 (short reflectance) band (B11), and a SWIR-2 (long reflectance) band (B12) for the computation of these pertinent indices. These indices include the normalized difference tillage index (NDTI), the soil tillage index (STI), the normalized difference vegetation index (NDVI), and the crop residue cover index (CRCI) (van Deventer et al., 1997; Carlson and Ripley,1997; Sullivan et al., 2006). Equations, literature references, and abbreviations for spectral indices used in the study are included in Table 1. Following the computation of spectral indices, we extracted the maximum values for each early-season period using the quality mosaic function in GEE within each of the 426 sample polygons.

We followed the two-step change detection approach to enhance class separability with the image composites created for each of the three time steps. In the first step, we subtracted the pre-sowing image composite from the end-of-harvest image composite to determine the changes that occurred in crop residue cover and surface texture due to CT and ST. To further enhance the separability between the three classes, we subtracted the post-sowing image composite from the image generated in the first step. This allowed us to further separate classes based on the changes that occur during the sowing process in ZT plots. Based on maximum class separability, we selected the NDTI and STI indices for further classification. Fig. S1 shows the enhancement in class separability observed at each step of the change detection analysis. The final composite generated in the second step of the change detection analysis is used for the development of a tillage classification model using random forest in GEE.

2.4. Model development and validation

We employed the smileRandomForest (RF) algorithm in GEE to classify ZT, CT and ST fields (Gorelick et al., 2017). Previous research has demonstrated that RF tends to achieve high classification accuracies compared to other active learning models like support vector machines (Mao et al., 2020; Liu et al., 2022). We developed our model using the image composites produced using the change detection analysis and field polygon data of ZT, CT, and ST fields collected for 2022. To quantify the improvement in accuracy that we achieve by using our two–step change detection methodology in a random forest model, we compared our two-step change detection RF model (named Model A) with three RF models that were separately trained using -early season

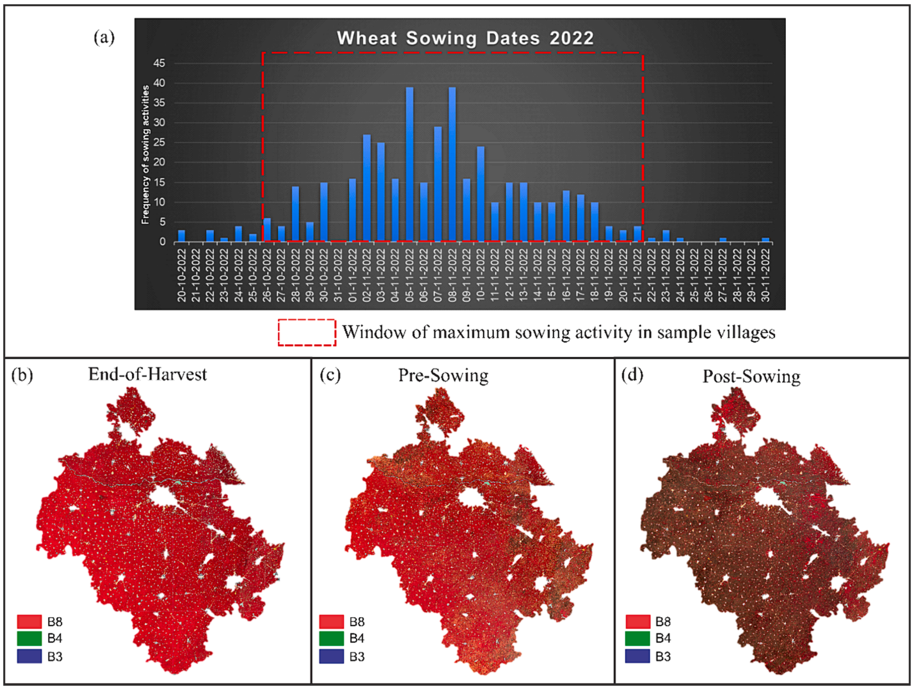

Fig. 2. (a) Bar diagram showing the distribution of wheat sowing activity across the sample villages reported in the ground survey. The red box highlights the window of maximum sowing activity and boundaries for pre and post-sowing periods. (b), (c) and (d) display the Sentinel-2 false colour composites (R: NIR, G: Red and B: Green) for end-of-harvest, pre-sowing and post-sowing time steps selected for change detection and classification. (2 column image). (For interpretation of the references to colour in this figure legend, the reader is referred to the web version of this article.)

Table 1
List of spectral indices used in this study.

Index Full Name	Abbreviation	Equation	Reference
Normalized Difference Tillage Index	NDTI	$\frac{\rho_{SWIR1} - \rho_{SWIR2}}{\rho_{SWIR1} + \rho_{SWIR2}}$	Pe˜na-Barrag´an et al., 2011
Soil Tillage Index	STI	$\frac{\rho_{SWIR1}}{\rho_{SWIR2}}$	Van Deventer et al., 1997
Crop Residue Cover Index	CRCI	$\frac{\rho_{GREEN} - \rho_{SWIR2}}{\rho_{GREEN} + \rho_{SWIR2}}$	Sullivan et al., 2006
Normalized Difference Vegetation Index	NDVI	$\frac{\rho_{NIR} - \rho_{RED}}{\rho_{NIR} + \rho_{RED}}$	Stroppiana et al., 2009

images from each of the three distinct time windows: the end of the harvest (Model B), pre-sowing (Model C) and post-sowing (Model D). To optimize the performance of the classifiers, we conducted hyper-parameter tuning. Through this process, we determined that the optimal number of decision trees for our random forest models were 250. Furthermore, we allocated a ratio of 60:10:30 for the training, hyper-parameter tuning, and validation phases of the classifier, respectively. We used a distinct set of validation polygons that were not used in training and served as an independent validation dataset. Furthermore, we maintained an equal proportion of ZT, CT and ST fields for model training and validation. We compared the model performance of all models for 2022 and selected the model with the highest accuracy for further analysis.

The best performing model (Model A) was then applied to imagery from the 2022, 2021, and 2020 post-monsoon seasons to estimate tillage adoption rates over the whole state of Punjab over three years. We believe that our model can be accurately applied through time, as previous studies that have mapped ZT have shown that random forest algorithms used to classify tillage practices are consistent through time (Azzari et al., 2019; Zhou et al., 2021). The same image processing steps to crate the two-step change detection model described above were applied to Sentinel-2 images for the years 2021 and 2020 before applying the classification model. To ensure that we only applied our classification algorithm to agricultural plots, we masked out non-agricultural classes using the ESRI 2020 Global Land Use Land Cover product (10 m) available in GEE (Karra et al., 2021). To exclude any permanent vegetation in plots, which may have been missed during the field data collection, we masked out any pixels that had mean NDVI values greater than 0.35 during the early time season window (Pinty and Verstraete, 1992). Fig. 3 gives an overview of the methodology followed to develop the tillage classification model as well as tillage adoption rate estimates for 2022.

2.5. Spatial and temporal trends in technology adoption

We calculated overall areas under ZT, CT, and ST in 2020, 2021, and 2022 across Punjab and for each district. We then examined values through time to understand whether areas under different tillage practices changed over the course of our study period. In addition, we examined areas (in ha) under each of the three tillage types using a three-year average to identify which districts planted the most and least area under ZT, CT, and ST.

3. Results

3.1. Validation of the model

Our study employed four distinct random forest (RF) models, to classify ZT, ST and CT adoption rates over the Indian state of Punjab. The performance of each model was evaluated based on several key metrics: commission error, omission error, user's accuracy, producer's accuracy, and the F1 Score. Fig. 4 provides each accuracy metric for each tillage class, with higher relative accuracies highlighted with darker boxes.

Model A, which used the two-step change detection method, performed best across all models. Model A had the highest producer's

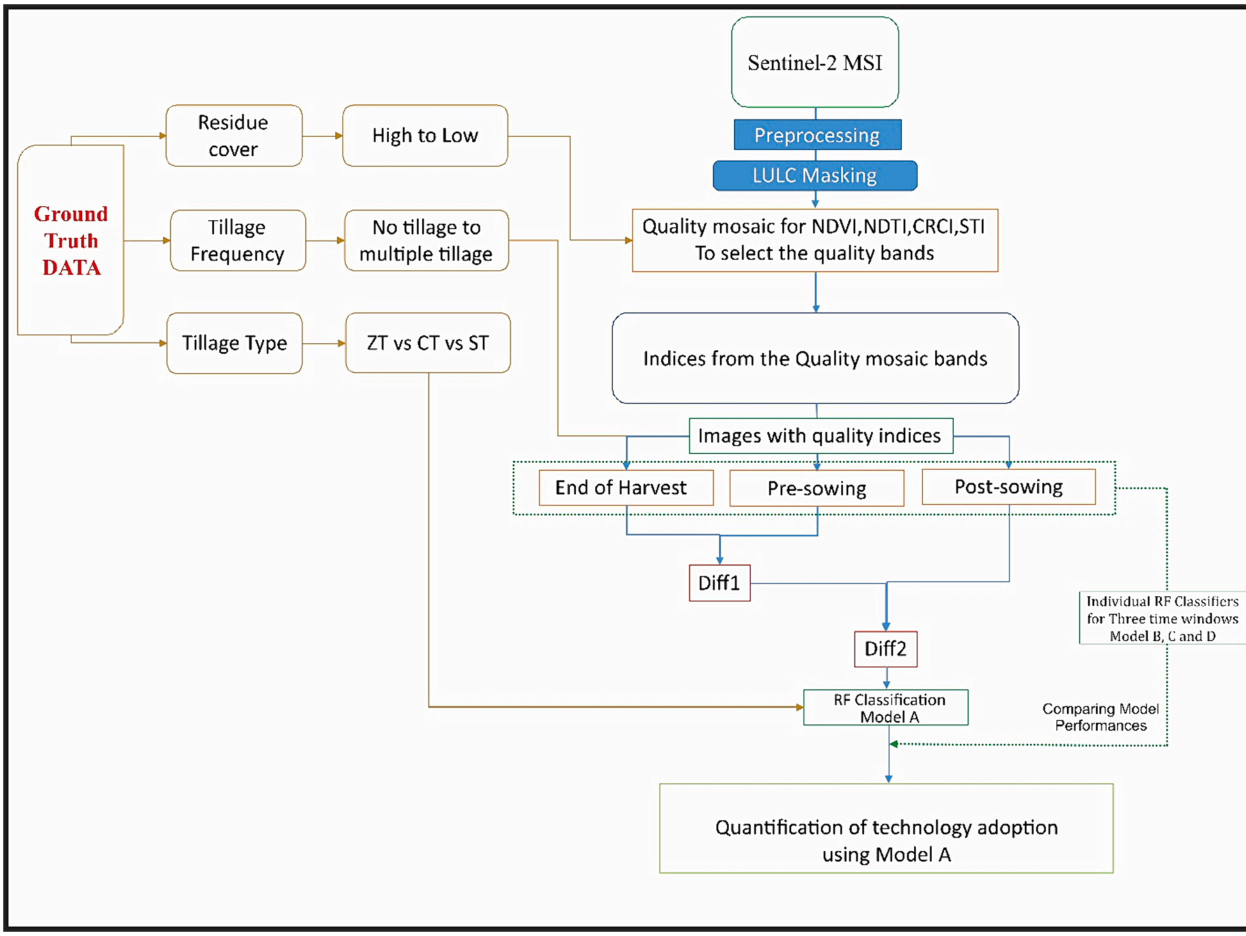

Fig. 3. Methodology design for the estimation of tillage adoption rates using Sentinel-2 imagery. (2 column image).

accuracy for ZT (92 %) and high user's accuracy across all classes (ZT: 70 %, ST: 87 %, and CT: 86 %). Model A also had consistently high F1 scores (with an average F1 score of 81 %), representing a good precision-recall balance, despite its relatively high omission errors for ST (20 %) and CT (25 %). In contrast, Model B, which was trained solely using end-of-harvest images, performed poorly with the highest commission (ZT: 16 %, ST: 13 %, and CT: 16 %) and omission errors (ZT: 29 %, ST: 31 %, and CT: 29 %), coupled with the lowest producer's accuracy and F1 scores across all classes (average F1: 70 %). These results suggest that Model B had significant challenges in both identifying classes correctly and avoiding false positives.

Model C, which was trained using images from the pre-sowing window, showed moderate performance considering user's accuracy and F1 scores, particularly for ST (72 % and 70 %, respectively) and CT (75 % for both). However, it also suffered from high omission errors, especially for ZT (31 %) and ST (32 %), and a commission error for CT (19 %). Model D, which was trained using post-sowing window images, had relatively low commission errors (13 % for ZT, 6 % for ST, and 15 % for CT). The particularly low commission error for ST (6 %) is a highlight, indicating that Model D has a high degree of specificity in identifying the ST class. While Model D exhibited high producer's accuracy for ZT (83 %) and user's accuracies for ST and CT (85 % and 80 %, respectively), it did not consistently perform well across all metrics. Specifically, it performed poorly considering omission errors for ZT and CT, (17 % and 25 %, respectively).

Fig. 5 gives the comparison between the overall accuracies of the four models. Model A provided the best balance between avoiding false positives and identifying actual instances of tillage activities. Therefore, Model A was applied to the 2021 and 2022 images for detecting the changes in tillage adoption through time.

3.2. Technology adoption rates across space and time

Our results revealed distinct tillage adoption trends for each tillage type over the three years from 2020 to 2022. Our results show a noticeable decrease in ZT adoption from 2020 to 2021, with the area under ZT reducing from 66,633 ha to 44,855 ha, a decline of approximately 33 %. However, the area under ZT increased in 2022, increasing to 53,191 ha, which is still lower than the initial 2020 area. ST showed a different pattern, with a substantial increase in the initial year, from 81,096 ha in 2020 to 104,730 ha in 2021, marking a significant rise of around 29 %. The area under ST dropped slightly in the next year, with 92,474 ha under ST in 2022, representing a modest decrease of about 12 %, which is still higher than the area under ST 2020. CT, on the other hand, has seen relatively stable values, with a slight decrease (4 %) in area in 2021 (46,427 ha) compared to 2020 (48,282 ha). There was a slight increase in area under CT in 2022 (49,308 ha), which is roughly a 6 % increase from the previous year and a 2 % increase from 2020. Among the 22 districts in Punjab, Hoshiarpur was found to have the highest adoption rate of ZT, with an average adoption rate of 57 %. Over the study period, prominent wheat and rice-producing districts like Bernala showed the highest ST adoption rate (62 %), followed by Moga (58 %) and Sangrur (57 %). Considering CT adoption rates, Fatehgarh Sahib had the highest adoption rate (27 %), whereas Hoshiarpur had the lowest adoption rate (19 %). Table 2 summarises the area (in ha) under each tillage type for all Punjab districts from 2020 to 2022. Fig. 6 shows the spatial distribution of field-level adoption of tillage technologies for 2020 to 2022 over Punjab.

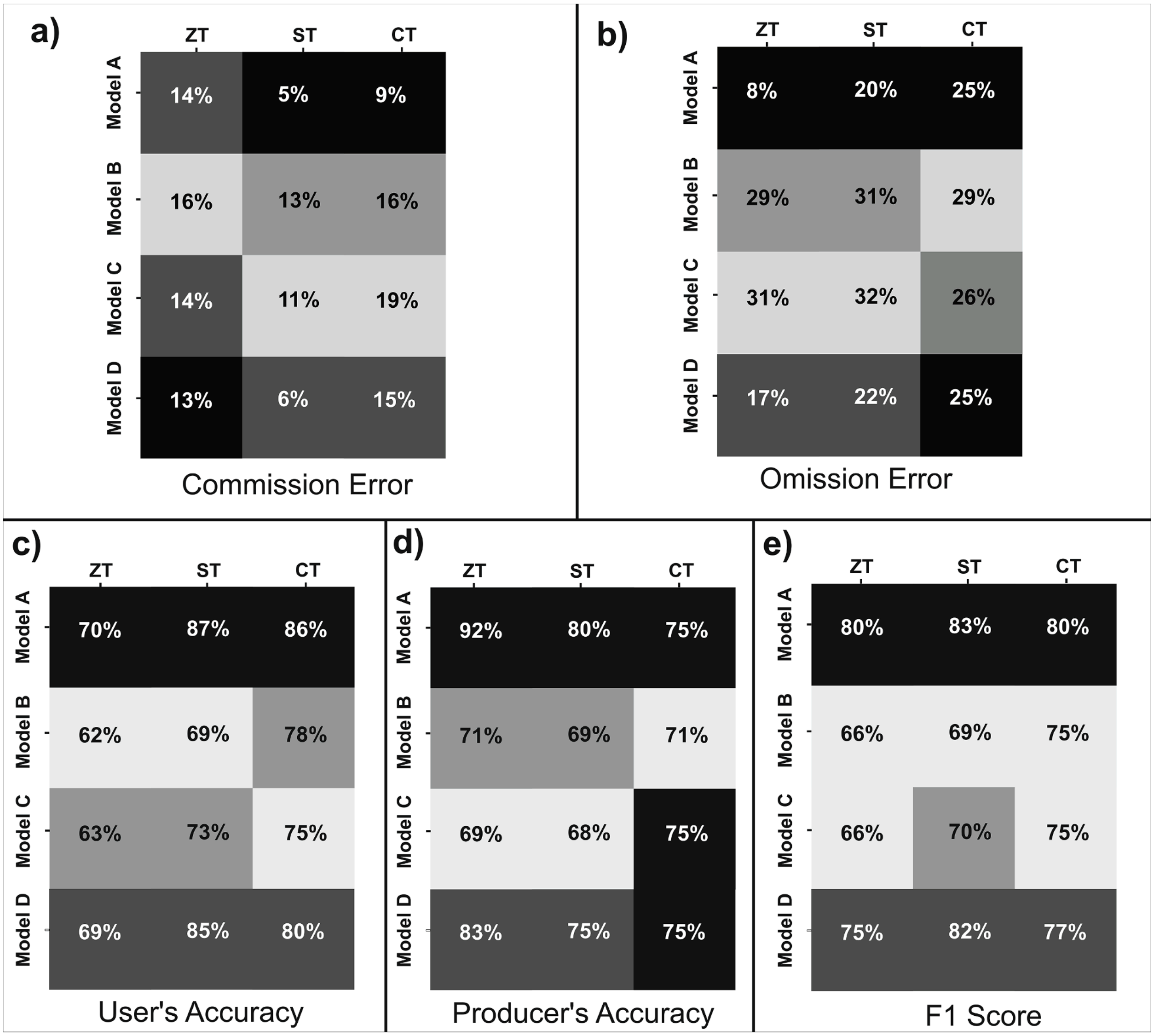

Fig. 4. The model comparison based on critical parameters: a) Commission Error, b) Omission Error, c) User's Accuracy, d) Producer's Accuracy, and e) the F1 Score. Rows represent the four models (models A-D) and columns represent each tillage class (ZT, ST, and CT). Darker colours represent more accurate values (2 column image).

4. Discussion

ZT is an important conservation agriculture technology, yet there is limited knowledge about its adoption extent and its impacts, particularly in developing countries. We examined the ability of Sentinel-2 imagery to detect ZT adoption at the field scale in heterogeneous, smallholder systems. We used change detection methods on early season imagery to distinguish among three different tillage types: ZT, ST, and CT. Until now, the detection of tillage practices has largely been constrained to binary models that differentiate only between ZT and CT (Azzari et al., 2019; Zhou et al., 2021; Liu et al., 2022). However, quantifying other tillage practices, such as ST, is important, given that it comprises a large proportion of agricultural area in smallholder systems such as India.

Our two-step change detection methodology significantly improves the RF classification across the three tillage classes. RF models trained using early season images only from one specific time window (end of harvest, pre and post sowing) were unable to obtain high classification accuracy across the three tillage classes. The best performing one time period model was Model D, which was trained using post-sowing images. In particular, it showed high specificity for ST, but did not perform as well when identifying ZT and CT. On the other hand, Model A, which was trained using the two-step early season change detection approach, was more balanced, demonstrating better overall precision and sensitivity, particularly for ZT and CT.

Model A performed well, with an overall accuracy of 81 %, which is higher than accuracies from previous studies that mapped ZT versus CT in multiple regions (Zheng et al., 2013; Azzari et al., 2019; Zhou et al., 2021; Liu et al., 2022). Our work shows that Sentinel-2 imagery, along with our novel change detection methodology, has the potential to map tillage practices in heterogeneous, smallholder systems.

Considering individual tillage types, the accuracies varied, with ZT having the best producer's accuracy (92 %), followed by ST (80 %) and then CT (75 %). These differences in accuracies are likely due to differences in the amount of crop residue typically left in the field when practising each tillage type. CT fields have no standing residue, as these residues are typically removed prior to tillage (typically through burning), and what residue remains is tilled within the soil when tillage machinery is used. This results in homogenous bare-field conditions within and across fields, which allows for higher classification accuracies. ZT, on the other hand, is characterized by crop residues remaining in the field even after ZT machinery is used, as residues are

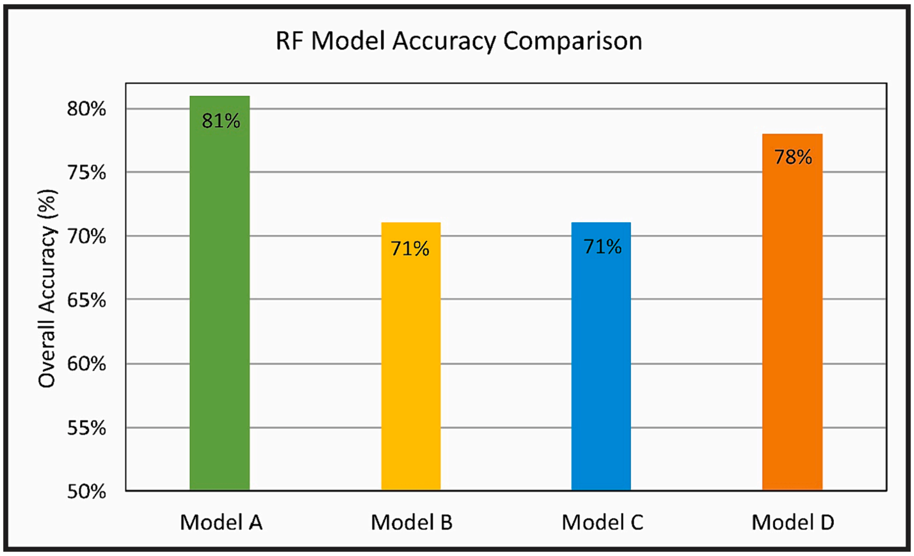

Fig. 5. Model performance comparison based on the overall classification accuracy (%).

Table 2
Model estimated area (ha) under ZT, ST and CT practices for districts of Punjab from 2022 to 2020.

Year	2020			2021			2022		
District	ZT (ha)	ST (ha)	CT (ha)	ZT (ha)	ST (ha)	CT (ha)	ZT (ha)	ST (ha)	CT (ha)
Bathinda	72,008	150,314	76,746	64,576	161,622	72,870	50,286	174,824	73,958
Faridkot	25,012	61,303	45,220	23,451	75,931	32,154	19,349	84,237	27,949
Fatehgarh Sahib	42,917	32,327	26,963	19,405	56,958	25,844	29,149	42,304	30,755
Hoshiarpur	142,726	44,996	38,651	116,403	64,553	45,414	130,805	53,573	41,996
Jalandhar	88,499	83,662	49,476	54,869	115,108	51,660	66,913	102,122	52,601
Kapurthala	58,258	53,849	32,728	36,519	71,114	37,203	44,429	63,545	36,862
Ludhiana	123,434	106,663	67,708	61,029	167,956	68,821	80,629	140,017	77,159
Mansa	50,585	103,682	50,099	43,181	111,146	50,039	32,847	118,167	53,352
Moga	50,841	113,214	50,789	29,083	138,888	46,872	34,235	124,140	56,469
Muktsar	46,402	120,919	74,462	45,382	139,187	57,214	47,858	139,871	54,054
Shahid Bhagat Singh Nagar	59,567	22,629	21,431	35,199	44,597	23,831	45,862	30,739	27,026
Barnala	25,100	80,923	34,968	16,980	94,433	29,579	18,506	86,174	36,311
Fazilka	104,735	95,534	69,019	83,654	119,588	66,046	107,326	107,309	54,654
Mohali	35,066	20,608	15,762	26,656	27,911	16,869	20,782	16,940	12,420
Patiala	95,408	124,534	72,252	50,372	170,021	71,801	71,523	131,895	88,777
Pathankot	26,738	16,566	12,547	21,241	21,864	12,746	24,433	18,258	13,160
Tarantaran	70,832	94,625	56,984	43,408	118,084	60,949	54,949	113,536	53,956
Amritsar	101,765	68,860	51,494	59,797	104,917	57,404	87,824	75,331	58,964
Sangrur	74,909	170,021	78,152	41,774	214,801	66,507	58,661	166,747	97,673
Gurdaspur	77,366	96,779	54,546	51,042	124,239	53,411	77,061	85,971	65,659
Rupnagar	52,634	17,777	18,602	29,673	39,692	19,648	36,579	28,265	22,622
Firozpur	41,128	104,333	63,604	33,110	121,454	54,502	30,201	130,467	48,397

not tilled into the soil during field preparation. Such contrasts in management practices result in distinctive spectral signatures that allow for the classification of ZT versus CT fields. However, ST plots exhibit characteristics resembling both ZT and CT fields because of the hybrid nature of field preparation. Though residues are not cleared prior to using the Super Seeder, ST fields appear bare after using the machinery, similar to CT fields, which often results in false-positive detections in the remote sensing model. Overall, we found that the modified change detection method we used did well in capturing differences in residue cover across the three tillage types early in the season. This is because the change between the monsoon crop harvest and pre-sowing of the winter crop captures residue cover prior to machinery use, which increas the class separability between CT fields (bare) versus ST or ZT plots (residue). In addition, the change between the pre-sowing and post-sowing time period captures textural changes in the field, such as the change in residue cover after tilling ST fields, which differentiates between ST (bare) and ZT (residue) fields (Luotamo et al., 2022; Quemada et al., 2018).

Our temporal analysis indicated a decrease in the adoption rates of ZT and CT and an increase in the adoption rate of ST from 2020 to 2021. However, we found the opposite pattern from 2021 to 2022, when ST adoption rates decreased slightly (Fig. 7). The sudden increase in ST and decrease in ZT and CT from 2020 to 2021 may be associated with post-lockdown measures following Covid-19. Amidst the COVID-19 pandemic in 2020, large labour migration increased the availability of agricultural labour in migrants' home states, including Punjab (Ravindra et al., 2022). This additional availability of labour may have incentivized farmers to forgo using CT. Additionally, the popularity of Supper Seeder machinery has seen a surge in Punjab in recent years with more and more farmers adopting ST practices (Krishna et al., 2022). Specifically, government subsidies and the availability of Super Seeder machinery may have motivated farmers to adopt ST over ZT. On the other hand, Punjab later faced large-scale farmer protests, reaching a peak in 2021, likely reducing available agricultural labour and accessibility to the super seeder machinery. In addition, the protests also spurred anti-government sentiment, resulting in increased residue

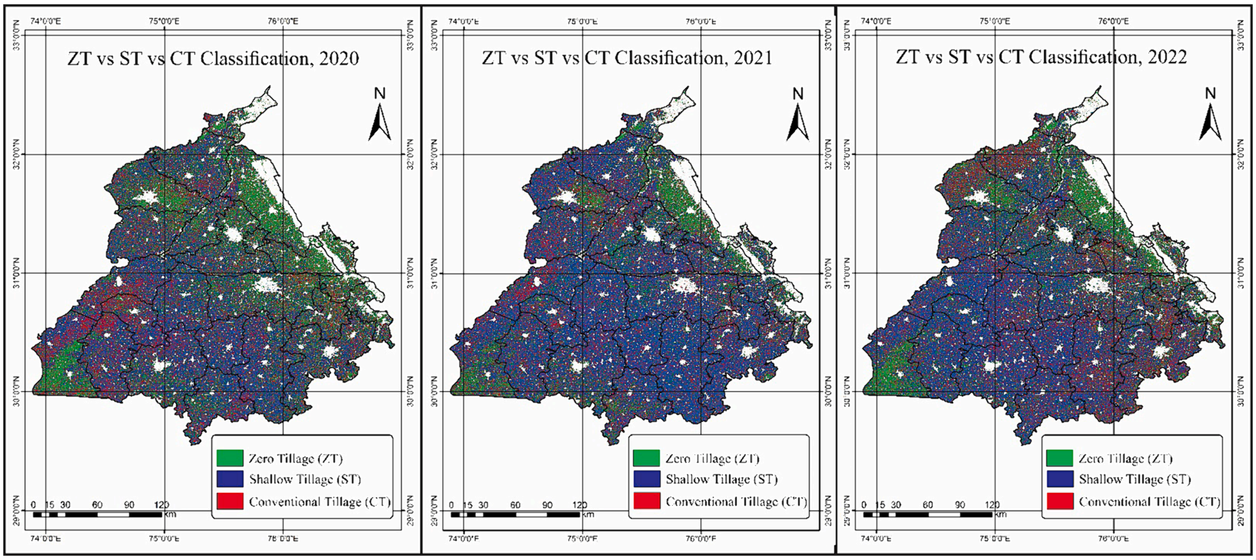

Fig. 6. Final model classification results depicting the spatial distribution of ZT, CT and ST adoption over the study area for (a) 2020, (b) 2021 and (c) 2022. (2 column image).

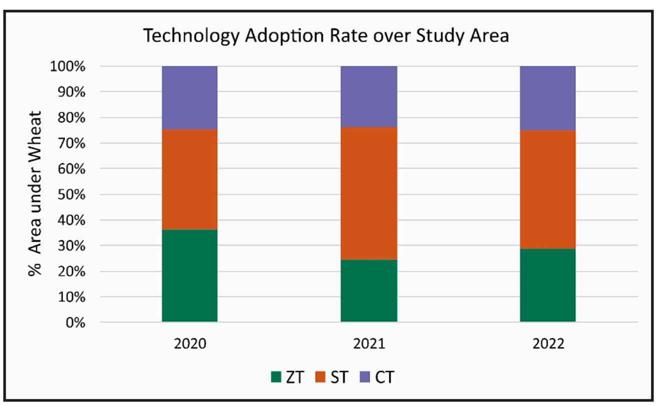

Fig. 7. Model estimated percente adoption of tillage technologies over the study area from 2020 to 2022. (2 column image).

burning, which was banned by the government. These factors may be responsible for farmers resorting back to ZT or CT practices as indicated by the slight increase in ZT and marginal increase in CT adoptions in 2022.. While we speculate the potential causes of tillage change through time, more work is needed to better understand the reasons for these detected temporal changes in tillage practices, likely through survey work that elucidates farmer decision-making. It is also possible that some of the trends we see may be driven by errors in our remote sensing analysis, which we elaborate on below.

While we achieved high accuracies, our remote sensing classification model had several limitations. First, the accuracy assessment results indicated that the model had higher commission errors for ZT and omission errors for ST and CT, which may have influenced estimates of their adoption rates, district and state scales. In particular, our confusion matrix (Fig. 4) suggests that there were misclassifications between CT and ST, likely given the similarity in bare field conditions after machinery use, and future work should focus on improving the separability of these classes. Second, it is possible that our remote sensing approach was limited in its ability to differentiate between tillage classes, given the short time frame of our study (3 years). This is because ZT helps to improve soil structure and fertility by preventing soil erosion as well as increasing the organic matter content of the soil, yet it is unlikely that these differences were captured in our remote sensing analysis as ZT has not been practised consistently in the same field for many years in our study region. Additionally Krishna et al. (2022) observed that ZT adoption is more likely among farmers situated more than 7.5 km from markets and those owning larger plots ($\geq$1.7 ha), particularly when equipped with a Rotavator, with the highest adoption rates in those farming over 18 ha. This research underscores the impact of market proximity, land size, and machinery ownership on the implementation of ZT practices. Future work that examines this region over longer time scales may be able to identify these changes, improving the accuracy of classification over time. Our method is also limited by the availability of cloud free images, as it uses images only over a short time period early in the growing season when there is often cloud cover and haze. Because of this, we were only able to apply our model to three years when cloud-free imagery were available (2020–2022). Future work is needed to address this issue by using microwave satellite data (eg. Sentinel-1) that can penetrate cloud cover. Finally, we did not account for crop type in our analysis, which may lead to further misclassifications. While most farmers in the region practice the rice–wheat cropping cycle, some farmers plant other crop types (e.g., sugarcane) and we were unable to mask out these fields as we did not have access to a crop type mask.

The findings of this study can significantly contribute to the development of agricultural policies and sustainable land management strategies. For example, by implementing a cost-effective and scalable approach to monitor and assess tillage practices over large areas, the present study contributes a potential way to examine adoption trends, helping to identify the factors that influence farmers' decisions to adopt ZT. By combining the spatiotemporal trends seen in the satellite data with on-the-ground survey and yield data, we can better identify the economic, social, and informational determinants of ZT adoption as well as the yield and economic impacts of ZT adoption (Ramulu et al., 2023; Krishna and Mkondiwa, 2023). In addition, satellite estimates of tillage practices can also be useful for quantifying carbon credits, which are associated with a reduction in carbon emissions or an increase in carbon sequestration. By estimating ZT adoption and its associated carbon sequestration, carbon market stakeholders, including governments and private firms, can more accurately quantify carbon offsets from this practice. Governments can use this information to create targeted incentives for farmers to adopt carbon-friendly ZT or other such practices. This policy support can stimulate greater participation in carbon markets and enhance their effectiveness in mitigating climate change. Furthermore, our methodology could empower farmers by providing them with the data needed to quantify their carbon offsets accurately.

This, in turn, can make it more attractive for farmers to engage in carbon market transactions, thereby generating additional income and incentivizing sustainable land management practices. (Thenkabail et al., 2010; Jackson Hammond et al., 2021).

5. Conclusion

Estimating ZT adoption at large spatiotemporal scales is crucial for promoting sustainable agriculture and designing supportive policies. Using Sentinel-2 imagery and Google Earth Engine, we developed a model that classified ZT, ST, and CT with overall accuracy and an average F1 score of 81 %. We applied this model to the state of Punjab from 2020 to 2022 and found that ST adoption rates have increased by 29 % in 2021 but showed 12 % decrease in 2022. On the other hand, area under ZT decreased significantly (33 %) in 2021 and did not recover back to its 2020 levels despite an increase in 2022. CT adoption rates remained steady across Punjab throughout our study period (2020–22). The use of remote sensing data offers a scalable approach to monitor tillage practices at large spatial and temporal scales. By leveraging these tools and findings, policymakers and agricultural stakeholders can make informed decisions to promote sustainable land management through the adoption of ZT.

CRediT authorship contribution statement

Monish Vijay Deshpande: Data curation, Formal analysis, Investigation, Methodology, Software, Writing – original draft. **Dhanyalekshmi Pillai:** Conceptualization, Funding acquisition, Supervision, Validation, Writing – review & editing, Investigation. **Vijesh V. Krishna:** Data curation, Writing – review & editing, Investigation. **Meha Jain:** Writing – review & editing, Investigation.

Declaration of competing interest

The authors declare that they have no known competing financial interests or personal relationships that could have appeared to influence the work reported in this paper.

Data availability

Data will be made available on request.

Acknowledgments

This study is supported by the project fund under grant T0193.01 provided by CIMMYT to D. Pillai (Ref: SEP-RO-2020-010). A project fund by the Max-Planck-Gesellschaft (Max Planck Partner Group, IISER Bhopal) has been utilized for the initial part of the study. The authors acknowledge the IISERB's High-Performance Computing (HPC) resources for the satellite data pre and post-processing and other computational support.

Appendix A. Supplementary material

Supplementary data to this article can be found online at https://doi.org/10.1016/j.jag.2024.103779.

References

Agricultural Statistics at a Glance, 2021. Agricultural statistics at a glance 2021, ministry of agriculture & farmers welfare department of agriculture, cooperation & farmers welfare, directorate of economics and statistics, government of India. https://eands.dacnet.nic.in/PDF/Agricultural%20Statistics%20at%20a%20Glance%20-%202021%20(English%20version).pdf (accessed May 04, 2023).

Azzari, G., Grassini, P., Edreira, J.I.R., Conley, S., Mourtzinis, S., Lobell, D.B., 2019. Satellite mapping of tillage practices in the north central US region from 2005 to 2016. Remote Sens. Environ. 221, 417–429. https://doi.org/10.1016/j.rse.2018.11.010.

Bricklemyer, R.S., Lawrence, R.L., Miller, P.R., Battogtokh, N., 2006. Predicting tillage practices and agricultural soil disturbance in north central Montana with landsat imagery. Agric. Ecosyst. Environ. 114, 210–216. https://doi.org/10.1016/j.agee.2005.10.005.

Carlson, T.N., Ripley, D.A., 1997. On the relation between NDVI, fractional vegetation cover, and leaf area index. Remote Sens. Environ. 62, 241–252. https://doi.org/10.1016/S0034-4257(97)00104-1.

Chabert, A., Sarthou, J.P., 2020. Conservation agriculture as a promising trade-off between conventional and organic agriculture in bundling ecosystem services. Agric. Ecosyst. Environ. 292, 106815.

Daughtry, C.S., Doraiswamy, P., Hunt Jr, E., Stern, A., McMurtrey Iii, J., Prueger, J., 2006. Remote sensing of crop residue cover and soil tillage intensity. Soil Tillage Res. 91, 101–108. https://doi.org/10.1016/j.still.2005.11.013.

Daughtry, C., Hunt Jr, E., McMurtrey III, J., 2004. Assessing crop residue cover using shortwave infrared reflectance. Remote Sens. Environ. 90 (126–134), 17. https://doi.org/10.1016/j.rse.2003.10.023.

Daughtry, C.S., Hunt Jr, E., Doraiswamy III, P., McMurtrey, J., 2005. Re- mote sensing the spatial distribution of crop residues. J. Agron. 97, 864–871. https://doi.org/10.2134/agronj2003.0291.

Ding, Y., Zhang, H., Wang, Z., Xie, Q., Wang, Y., Liu, L., Hall, C.C., 2020. A comparison of estimating crop residue cover from sentinel-2 data using empirical regressions and machine learning methods. Remote Sens. 12, 1470 https://doi.org/10.3390/RS12091470.

El-Shater, T., Yigezu, Y.A., Mugera, A., Piggin, C., Haddad, A., Khalil, Y., Loss, S., Aw-Hassan, A., 2016. Does zero tillage improve the livelihoods of smallholder cropping farmers? J. Agric. Econ. 67, 154–172.

El-Shater, T., Mugera, A., Yigezu, Y.A., 2020. Implications of adoption of zero tillage (zt) on productive efficiency and production risk of wheat production. Sustainability 12, 3640. https://doi.org/10.3390/su12093640.

Gao, L., Zhang, C., Yun, W., Ji, W., Ma, J., Wang, H., Li, C., Zhu, D., 2022. Mapping crop residue cover using adjust normalized difference residue index based on sentinel-2 msi data. Soil Tillage Res. 220, 105374 https://doi.org/10.1016/j.still.2022.105374.

Gorelick, N., Hancher, M., Dixon, M., Ilyushchenko, S., Thau, D., Moore, R., 2017. Google earth engine: planetary-scale geospatial analysis for everyone. Remote Sens. Environ. 202, 18–27. https://doi.org/10.1016/j.rse.2017.06.031.

Hively, W.D., Lamb, B.T., Daughtry, C.S., Shermeyer, J., McCarty, G.W., Quemada, M., 2018. Mapping crop residue and tillage intensity using worldview-3 satellite shortwave infrared residue indices. Remote Sens. 10 (1657), 18. https://doi.org/10.3390/rs10101657.

Immitzer, M., Vuolo, F., Atzberger, C., 2016. First experience with sentinel- 2 data for crop and tree species classifications in central Europe. Remote Sens. 8, 166 https://doi.org/10.3390/rs8030166.

Jackson Hammond, A.A., Motew, M., Brummitt, C.D., DuBuisson, M.L., Pinjuv, G., Harburg, D.V., Campbell, E.E., Kumar, A.A., 2021. Implementing the soil enrichment protocol at scale: opportunities for an agricultural carbon market. Front. Clim. 64 https://doi.org/10.3389/fclim.2021.686440.

Jain, M., Srivastava, A.K., Joon, R.K., McDonald, A., Royal, K., Lisaius, M.C., Lobell, D.B., 2016. Mapping smallholder wheat yields and sowing dates using micro-satellite data. Remote Sens. 8, 860 https://doi.org/10.3390/rs8100860.

Jat, M.L., Chakraborty, D., Ladha, J.K., Rana, D.S., Gathala, M.K., Mc- Donald, A., Gerard, B., 2020. Conservation agriculture for sustainable intensification in south Asia. Nat. Sustain 3, 336–343. https://doi.org/10.1038/s41893-020-0500-2.

Karra, K., Kontgis, C., Statman-Weil, Z., Mazzariello, J.C., Mathis, M., Brumby, S.P., 2021. Global land use/land cover with sentinel 2 and deep learning. In: 2021 IEEE International Geoscience and Remote Sensing Symposium IGARSS, pp. 4704–4707.

Kassam, A., Friedrich, T., Shaxson, F., Pretty, J., 2009. The spread of conser- vation agriculture: justification, sustainability and uptake. Int. J. Agric. Sustain. 7, 292–320. https://doi.org/10.3763/ijas.2009.0477.

Krishna, V.V., Keil, A., Jain, M., Zhou, W., Jose, M., Surendran-Padmaja, S., Barba-Escoto, L., Jat, M., Erenstein, O., et al., 2022. Conservation agriculture benefits Indian farmers, but technology targeting needed for greater impacts. Front. Agron. 4, 772732.

Krishna, V.V., Mkondiwa, M., 2023. Economics of crop residue management. Annu. Rev. Resour. Econ. 15, 19–39.

Kubitza, C., Krishna, V.V., Schulthess, U., Jain, M., 2020. Estimating adoption and impacts of agricultural management practices in developing countries using satellite data. A scoping review. ASD 40, 1–21. https://doi.org/10.1007/s13593-020-0610-2.

Lal, R., 2005. World crop residues production and implications of its use as a biofuel. Environ. Int. 31 (575–584), 19. https://doi.org/10.1016/j.envint.2004.09.005.

Lewis, D., Yao, H., Fridgen, J., Kincaid, R., 2006. Investigation on the potential of using ASTER image for corn plant residue coverage estimation in three Indiana counties. IEEE Int. Symp. Geosci. Remote Sens. 2006, 2092–2094. https://doi.org/10.1109/IGARSS.2006.541.

Liu, Y., Rao, P., Zhou, W., Singh, B., Srivastava, A.K., Poonia, S.P., Van Berkel, D., Jain, M., 2022. Using sentinel-1, sentinel-2, and planet satellite data to map field-level tillage practices in smallholder systems. PLoS One 17, e0277425. https://doi.org/10.1371/journal.pone.0277425.

Luotamo, M., Yli-Heikkil ̈a, M., Klami, A., 2022. Density estimates as representations of agricultural fields for remote sensing-based monitoring of tillage and vegetation cover. Appl. Sci. 12, 679 https://doi.org/10.3390/app12020679.

Main-Knorn, M., Pflug, B., Louis, J., Debaecker, V., M ̈uller-Wilm, U., Gascon, F., 2017. Sen2cor for sentinel-2, in: Image and Signal Processing for Remote Sensing XXIII, SPIE. pp. 37–48. doi: 10.1117/12.2278218.

Mao, W., Lu, D., Hou, L., Liu, X., Yue, W., 2020. Comparison of machine-learning methods for urban land-use mapping in Hangzhou city, China. Remote Sens. 12, 2817 https://doi.org/10.3390/rs12172817.

Pe˜na-Barrag´an, J.M., Ngugi, M.K., Plant, R.E., Six, J., 2011. Object-based crop identification using multiple vegetation indices, textural features and crop phenology. Remote Sens. Environ. 115, 1301–1316.

Pinty, B., Verstraete, M., 1992. Gemi: a non-liCOVID index to monitor global vegetation from satellites. Vegetatio 101, 15–20.

Quemada, M., Hively, W., Daughtry, C., Lamb, B., Shermeyer, J., 2018. Improved crop residue cover estimates obtained by coupling spectral indices for residue and moisture. Remote Sens. Environ. 206, 33–44. https://doi.org/10.1016/j.rse.2017.12.012.

Ramulu, C., Pateriya, R.N., Naik, M.A., Vishwakarma, D.K., Kuriqi, A., Al-Ansari, N., Alataway, A., Dewidar, A.Z., Mattar, M.A., 2023. A residue management machine for chopping paddy residues in combine harvested paddy field. Sci. Rep. 13 (5077), 20. https://doi.org/10.1038/s41598-023-32148-9.

Ravindra, K., Singh, T., Mor, S., 2022. Covid-19 pandemic and sudden rise in crop residue burning in India: issues and prospects for sustainable crop residue management. Environ. Sci. Pollut. Res. 29, 3155–3161.

Serbin, G., Daughtry, C.S., Hunt Jr, E.R., Brown, D.J., McCarty, G.W., 2009. Effect of soil spectral properties on remote sensing of crop residue cover. Soil Sci. Soc. Am. J. 73, 1545–1558. https://doi.org/10.2136/sssaj2008.0311.

Sharma, V., Irmak, S., Kilic, A., Sharma, V., Gilley, J.E., Meyer, G.E., Knezevic, S.Z., Marx, D., 2016. Quantification and mapping of surface residue cover for maize and soybean fields in south central Nebraska. Trans. ASABE 59, 925–939. https://doi.org/10.5194/angeo-28-367-2010.

Singh, V., Gupta, R.K., Kahlon, M., Toor, A., Singh, K., Al-Ansari, N., Mattar, M.A., 2023. Effect of different tillage and residue management options on soil water transmission and mechanical behavior. Land 12, 1895. https://doi.org/10.13031/trans.59.11489.

Stewart, B., Asfary, A., Belloum, A., Steiner, K., Friedrich, T., 2008. Conservation agriculture for sustainable land management to improve the livelihood of people in dry areas. Arab Center for the Studies of Arid Zones and Dry Lands and the German Agency for Technical Cooperation, Damascus, Syria and Eschborn, Germany, www.fao.org/ag/ca/doc/CA% 20Workshop% 20procedding, 08–08.

Stroppiana, D., Boschetti, M., Brivio, P.A., Bocchi, S., 2009. Plant nitrogen concentration in paddy rice from field canopy hyperspectral radiometry. Field Crops Res. 111, 119–129.

Sullivan, D.G., Truman, C.C., Schomberg, H.H., Endale, D.M., Strickland, T.C., 2006. Evaluating techniques for determining tillage regime in the southeastern coastal plain and piedmont. J. Agron. 98, 1236–1246. https://doi.org/10.2134/agronj2005.0294.

Thenkabail, P.S., Hanjra, M.A., Dheeravath, V., Gumma, M., 2010. A holistic view of global croplands and their water use for ensuring global food security in the 21st century through advanced remote sensing and non-remote sensing approaches. Remote Sens. 2, 211–261. https://doi.org/10.3390/rs2010211.

Tiwari, D., Kaur, M., Dhaliwal, R., 2010. Constraints faced by the practicing farmers in adoption of zero tillage technology in Punjab. Indian J. Extension Educ. 46, 101–105.

Van Deventer, A., Ward, A., Gowda, P., Lyon, J., 1997. Using thematic mapper data to identify contrasting soil plains and tillage practices. Photogramm. Eng. Remote Sens. 63, 87–93.

Watts, J.D., Powell, S.L., Lawrence, R.L., Hilker, T., 2011. Improved classification of conservation tillage adoption using high temporal and synthetic satellite imagery. Remote Sens. Environ. 115, 66–75. https://doi.org/10.1016/j.rse.2010.08.005.

Xie, Q., Dash, J., Huete, A., Jiang, A., Yin, G., Ding, Y., Peng, D., Hall, C.C., Brown, L., Shi, Y., et al., 2019. Retrieval of crop biophysical parameters from sentinel-2 remote sensing imagery. Int. J. Appl. Earth Obs. Geoinf. 80, 187–195. https://doi.org/10.1016/j.jag.2019.04.019.

Zheng, B., Campbell, J.B., de Beurs, K.M., 2012. Remote sensing of crop residue cover using multi-temporal landsat imagery. Remote Sens. Environ. 117, 177–183.

Zheng, B., Campbell, J.B., Shao, Y., Wynne, R.H., 2013. Broad-scale monitoring of tillage practices using sequential landsat imagery. Soil Sci. Soc. Am. J. 77, 1755–1764. https://doi.org/10.2136/sssaj2013.03.0108.

Zheng, B., Campbell, J.B., Serbin, G., Galbraith, J.M., 2014. Remote Sens. of crop residue and tillage practices: present capabilities and future prospects. Soil Tillage Res. 138, 26–34. https://doi.org/10.1016/j.rse.2011.09.016.

Zhou, W., Rao, P., Jat, M.L., Singh, B., Poonia, S., Bijarniya, D., Kumar, M., Singh, L.K., Schulthess, U., Singh, R., et al., 2021. Using sentinel-2 to track field-level tillage practices at regional scales in smallholder systems. Remote Sens. 13, 5108 https://doi.org/10.3390/rs13245108.